



Universiteit  
Leiden  
The Netherlands

## **Zebrafish as research model to study Gaucher disease: Insights into molecular mechanisms**

Lelieveld, L.T.

### **Citation**

Lelieveld, L. T. (2020, October 20). *Zebrafish as research model to study Gaucher disease: Insights into molecular mechanisms*. Retrieved from <https://hdl.handle.net/1887/137851>

Version: Publisher's Version

License: [Licence agreement concerning inclusion of doctoral thesis in the Institutional Repository of the University of Leiden](#)

Downloaded from: <https://hdl.handle.net/1887/137851>

**Note:** To cite this publication please use the final published version (if applicable).

Cover Page



Universiteit Leiden



The handle <http://hdl.handle.net/1887/137851> holds various files of this Leiden University dissertation.

**Author:** Lelieveld, L.T.

**Title:** Zebrafish as research model to study Gaucher disease: Insights into molecular mechanisms

**Issue date:** 2020-10-20

# CHAPTER 3

## Pharmacological modulation of glycosidases in zebrafish



Adapted from: FEBS J. 2019 Feb;286(3):584-600  
Kuo CL, Kallemeijn WW, Lelieveld LT, Mirzaian M, Zoutendijk I, Vardi A, Futerman AH, Meijer AH, Spalink HP, Overkleeft HS, Aerts JMFG and Artola M.  
• In vivo inactivation of glycosidases by conduritol B epoxide and cyclophellitol as revealed by activity-based protein profiling.

and from: JACS. 2019 Mar 13;141(10):4214-4218  
Artola M, Kuo CL, Lelieveld LT, Rowland RJ, van der Marel GA, Codée JDC, Boot RG, Davies GJ, Aerts JMFG and Overkleeft HS.  
• Functionalized Cyclophellitols Are Selective Glucocerebrosidase Inhibitors and Induce a Bona Fide Neuropathic Gaucher Model in Zebrafish.

## Abstract

**Z**ebrafish, and especially their developing off-spring, offer attractive features to study the molecular basis of genetic disorders as well as pharmacological intervention in a whole organism. Gaucher disease (GD) is a common lysosomal storage disorder, characterized by a defect in the enzyme glucocerebrosidase (GCase or GBA, official gene name: *GBA*) which hydrolyses the lipid glucosylceramide in lysosomes. Studying GD in an animal model has been hampered by the premature death of mammals with a complete genetic abrogation of GBA. Therefore, on-demand GBA deficiency has been induced chemically, by treatment of animals with the mechanism-based irreversible GBA inhibitors conduritol B epoxide (CBE) or cyclophellitol (CP). Zebrafish larvae are used in this chapter to study the *in vivo* target engagement of CBE and CP and compare the results to values obtained from cultured human cells. Only at significantly higher CBE concentrations, non-lysosomal glucosylceramidase (GBA2) and lysosomal  $\alpha$ -glucosidase were identified as major off-targets both in cells and zebrafish larvae. CP was found to inactivate GBA and GBA2 with equal affinity and is therefore not suitable to generate genuine GD-like models. New CP derivatives, functionalized with a bulky hydrophobic moiety at C8, were validated as potent and selective GBA inhibitors in cultured cells and developing zebrafish larvae. Moreover, these CP analogues selectively inhibit GBA in the brain of adult zebrafish. Overall, this chapter demonstrates the applicability of enzymatic assays and ABPs as tools to study zebrafish glycosidase enzymes as well as the attractive features of the zebrafish animal model for evaluating drug potency, specificity and biodistribution, in particular brain permeability.

## Introduction

The lysosomal enzyme glucocerebrosidase (GCase or GBA, EC 3.2.1.45) is a retaining  $\beta$ -glucosidase that degrades the glycosphingolipid, glucosylceramide (GlcCer). Inherited deficiency of GBA is the cause of autosomal recessive Gaucher disease (GD)<sup>1</sup>. Most GD patients display heterogeneous symptoms including spleen and liver enlargement, bone deterioration, anaemia, leukopenia, and thrombocytopenia, while some patients also develop fatal neurological symptoms<sup>2</sup>.

Research on GD has been hampered by the premature death of mice with a complete genetic abrogation of GBA. Therefore, on-demand GBA deficiency have been generated by treatment of animals with conduritol B epoxide (CBE **1**, **Figure 1A**)<sup>3-5</sup>. CBE is a cyclitol epoxide that covalently and irreversibly reacts with the catalytic nucleophile of GBA and thus inactivates the enzyme irreversibly (**Figure 1B**). The crystal structure of GBA with bound CBE confirmed the covalent linkage of the compound to the catalytic nucleophile Glu 340<sup>6,7</sup>. Building on the initial work by Kanfer and co-workers, a regimen using different doses of CBE has been established to generate a phenotypic copy of neuronopathic GD in mice<sup>4,6-8</sup>. This pharmacological model is widely used to study the nature of neuropathology resulting from GBA deficiency, including Parkinsonism<sup>9-11</sup>.

A major advantage of CBE's pharmacological use in cultured cells and mice is its tunability: the extent of GBA inactivation can be adjusted by variation of the inhibitor concentration and/or exposure time<sup>4</sup>. However, distinct treatment regimens across studies have been reported: exposure of cells ranging from 50  $\mu$ M to 100 mM CBE for 2 hours up to 60 days<sup>12-18</sup> and daily exposure of mice from 25 to 300 mg per kg body weight during 2 hours up to 36 days<sup>4</sup>. The use of a high CBE concentration raises concerns about specificity since the compound has been reported to inhibit other glycosidases than GBA at high concentrations. Examples are *in vitro* inhibition of retaining  $\alpha$ -glucosidases (EC 3.2.1.20)<sup>19-21</sup>, *in vitro*<sup>22</sup> and *in situ*<sup>23</sup> cell inhibition of the non-lysosomal glucosylceramidase (GBA2, EC 3.2.1.45), and inhibition of the lysosomal  $\beta$ -glucuronidase (GUSB, EC 3.2.1.31) in mice<sup>24</sup>. The reactivity of CBE towards both  $\beta$ - and  $\alpha$ -glucosidases can be explained by the C2-symmetry found in its structure<sup>25</sup> (**Figure 1A**), which allows reaction with the catalytic nucleophile of both classes of enzymes. Another structurally related cyclitol epoxide, cyclophellitol (CP **2**, **Figure 1A**), is a structurally closer  $\beta$ -glucose mimic and inhibits GBA with far higher affinity than CBE<sup>26,27</sup>. It exhibits selectivity over  $\alpha$ -glucosidases due to the C5-hydroxymethyl group<sup>26-28</sup>, and was also shown to induce Gaucher phenotypes in mice<sup>26</sup>. However, its reactivity *in vivo* towards GBA2 and other glycosidases is unknown. Recently, CP derivatives have been functionalized with a fluorescent substituent at C8 (**3a-e**, **Figure 1A**). The generated cyclophellitol-epoxide activity-based probe (ABP **3**) showed very potent and selective reactivity towards GBA and was used to visualize and monitor GBA activity *in vitro*, *in situ* and *in vivo*<sup>28,29</sup>.

Next, a configured cyclophellitol-aziridine tagged with a fluorophore was developed which enabled labelling of all retaining  $\beta$ -glucosidases (ABP **4**)<sup>30</sup>. To date, a library of ABPs is available labelling a range of retaining glycosidases (**Figure 1A**), including ABPs targeting  $\beta$ -glucuronidase (GUSB, ABP **5**<sup>31</sup>) and  $\alpha$ -glucosidase (GAA and GANAB, ABP **6**<sup>32</sup>) as well as ABPs functionalized with different fluorophores (**Figure 1C**). It has been previously established that the CP derivative, functionalized with a BODIPY group, does not penetrate the brain sufficiently<sup>29</sup>. Changing the fluorescent BODIPY substituent to a simple, hydrophobic moiety at C8 (inhibitors **3d** and **3e**, **Figure 1C**) is thought to preserve the high potency and selectivity of the inhibitor, while improving GBA inactivation in the brain. This would make them suitable for generating chemically-induced neuropathic Gaucher disease models.

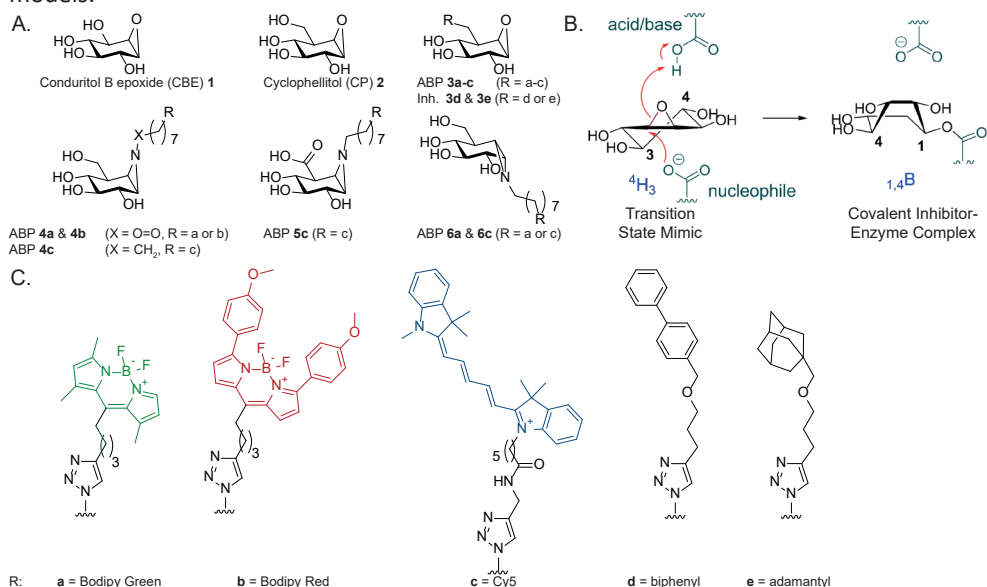


**Figure 1 | Overview of chemical structures used in this study**

**(A)** Top panel: Chemical structures of Conduritol B epoxide (CBE), cyclophellitol (CP), CP-configured ABPs (ABP **3a-c**) and CP-derived inhibitors (**3d,e**). Lower panel: ABP labelling GBA and GBA2 (ABP **4a-c**), GUSB (ABP **5c**) and GAA and GANAB (ABP **6a** and **6c**) **(B)** Reaction mechanism of CBE binding to  $\beta$ -glucosidase. **(C)** Chemical structures of R-groups in A: Bodipy Green (a), Bodipy Red (b), Cy5 (c), biphenyl (d) and adamantyl moiety (e).

This chapter describes a systematic study of the *in vitro* and *in vivo* potency and selectivity of CBE, CP and CP derivatives using cultured cells and developing zebrafish larvae. Both enzymatic assays, employing specific fluorogenic substrates, and competitive activity-based protein profiling (cABPP) using a library of ABPs (**Figure 1A**, ABPs **3-6**) are used. Finally, two CP derivatives, one with a BODIPY-substituent at C6 (compound **3a**) and the other with a hydrophobic group (compound **3e**), were administered to adult zebrafish to assess the penetration and target engagement of these inhibitors in the brain.

## Results

### A competitive ABPP method to determine GBA target engagement of CBE and CP

ABP **4c** was used in a competitive ABPP method to assess the irreversible occupancy of the catalytic nucleophile of GBA after pre-incubation with CBE **1** or CP **2**. As a validation, competition of ABP labelling by CBE and CP was compared to the loss of GBA activity measured using the artificial fluorogenic substrate, 4-methylumbelliferyl- $\beta$ -glucoside<sup>33</sup>. For this, recombinant human GBA (rGBA) was pre-incubated with CBE across a range of concentrations at 37 °C for 0, 30 and 180 minutes<sup>34</sup>. Subsequent labelling of GBA by ABP **4c** enabled quantification by SDS-PAGE and fluorescence scanning. IC<sub>50</sub> values (concentrations of inhibitor yielding a 50% reduction of ABP **4c** labelling) were determined and found to be 26.6  $\mu$ M at 30 min CBE preincubation, and 2.30  $\mu$ M at 180 min pre-incubation (**Figure 2A**). These values match the ones determined by measurement of residual enzymatic activity of the GBA assay (**Figure 2A**, lower right panel), validating the competitive ABPP methodology. Next, CP was comparably studied using rGBA and its IC<sub>50</sub> values determined by cABPP were 0.15  $\mu$ M at 30 min pre-incubation and 0.03  $\mu$ M at 180 min pre-incubation, comparable to values determined by enzymatic assay (**Figure 2B**).

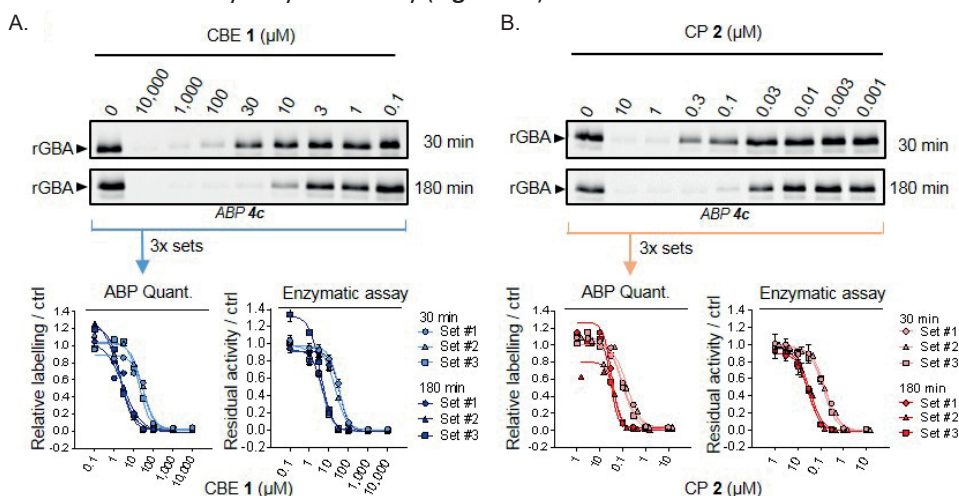


**Figure 2 | Effect of pre-incubation with CBE or CP on ABP labelling of recombinant GBA.**

(A) Representative gel images of rGBA pre-incubated with CBE (10,000–0.1  $\mu$ M) for 30 min or 180 min and fluorescently labelled with ABP **4c**. Fluorescent signals were quantified and normalized to the untreated sample (ctrl, 0  $\mu$ M CBE) (bottom left) and compared to the inhibition curves obtained with enzymatic assay (bottom right). (B) Same as A, with CP at 10–0.001  $\mu$ M. Error ranges in enzymatic assay =  $\pm$  SD, n = 3 (technical replicates).

### Selectivity of CBE and CP in cultured cells

Next, the targets of CBE and CP were evaluated in intact cultured human cells and zebrafish larvae. These biological materials contain besides GBA the candidate off-target glycosidases: GBA2,  $\alpha$ -glucosidases (GAA and GANAB), and lysosomal  $\beta$ -glucuronidase GUSB. For each of these enzymes ABPs have been designed, and enzymatic activity assays with fluorogenic substrates established<sup>30–32</sup>. Of note, ABP **4** allows simultaneous visualization of active GBA (58–66 kDa) and GBA2 (110 kDa) following SDS-PAGE analysis.



First, HEK293T cells overexpressing GBA2 were exposed to different concentrations of CBE (0.1  $\mu\text{M}$ –10 mM) or CP (0.001 – 10  $\mu\text{M}$ ) for 24 h. The residual amount of GBA, GBA2, GAA, GANAB and GUSB that can still be labelled with the appropriate ABPs (**Figure 1C**) was determined in the exposed cell lysates (**Figure 3A** and **D** for CBE and CP respectively).

For CBE, competitive ABPP showed that besides GBA, all other candidate off-target enzymes are inactivated but with marked lower affinity: GBA ( $\text{IC}_{50} = 0.59 \mu\text{M}$ ), GBA2 ( $\text{IC}_{50} = 315 \mu\text{M}$ ), GAA ( $\text{IC}_{50} = 249 \mu\text{M}$ ), GANAB ( $\text{IC}_{50} = 2900 \mu\text{M}$ ) and GUSB ( $\text{IC}_{50} = 857 \mu\text{M}$ ) (**Figure 3B**, **Supplementary Figure 1A** and **Supplementary Table 1**). Comparable results were obtained by determination of residual enzyme activities: GBA ( $\text{IC}_{50} = 0.33 \mu\text{M}$ ), GBA2 ( $\text{IC}_{50} = 272 \mu\text{M}$ ), GAA ( $\text{IC}_{50} = 309 \mu\text{M}$ ), GANAB ( $\text{IC}_{50} = 1580 \mu\text{M}$ ) and GUSB ( $\text{IC}_{50} = 607 \mu\text{M}$ ) (**Figure 3C** and **Supplementary Figure 1B**). CP is a much more potent inhibitor of GBA<sup>26</sup> and reported to inhibit poorly  $\alpha$ -glucosidases *in vitro*<sup>27</sup>. However, the *in vivo* reactivity of CP towards other glycosidases has not been thoroughly investigated. To compare the selectivity windows of CP to the ones of CBE, the concentration range of CP was chosen at 0.001–10  $\mu\text{M}$  for cultured cells. As determined by the competitive ABPP method, CP was found to inhibit GBA2 on a par with GBA in cells overexpressing GBA2 upon incubation with varying inhibitor concentrations (0.1–10  $\mu\text{M}$  CP) for 24 hours (**Figure 3D-F**).

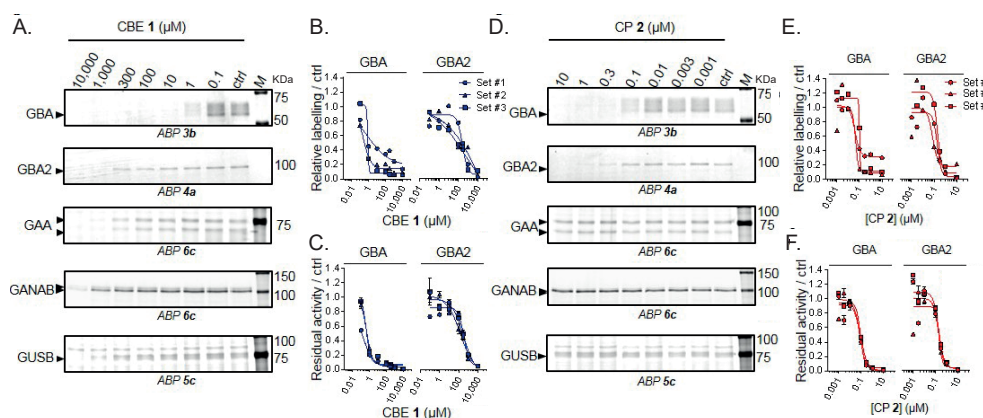


**Figure 3 | *In vivo* glycosidase targets of CBE and CP in cultured cells**

(A, D) Representative gel images (1 set from  $n = 3$  biological replicates) showing fluorescent ABP labelling of GBA, GBA2, GAA, GANAB, and GUSB in lysates of cells treated *in vivo* for 24 h with CBE (A) and CP (D) respectively. (B, E) Quantification of relative ABP labelling of GBA and GBA2 in lysates of cells treated *in vivo* for 24 h with CBE (B) and CP (E) respectively. (C, F) Residual activities of GBA and GBA2 in cell lysates treated *in vivo* with CBE (C) and CP (F). Error ranges =  $\pm$  SD,  $n = 3$  (technical replicates).

$\text{IC}_{50}$  values of CP for blocking ABP labelling were 0.063  $\mu\text{M}$  for GBA and 0.154  $\mu\text{M}$  for GBA2 (**Figure 3E** and **Supplementary Table 1**), which was comparable to results obtained by determination of residual enzymatic activities of GBA and GBA2 measured with the fluorogenic 4Mu substrate (**Figure 3F**). No reduction of ABP labelling of GAA, GANAB and GUSB was observed in lysates of cells incubated for 24 h up to 10  $\mu\text{M}$  of CP (**Figure 3D**). The apparent  $\text{IC}_{50}$  values of CP for the other glycosidase enzymes exceeded at least 10  $\mu\text{M}$  (**Supplementary Table 1** and ref.<sup>35</sup>).



***In vivo* targets of CBE and CP in zebrafish larvae**

Next, the *in vivo* target engagement of CBE and CP was studied in intact zebrafish larvae. Fertilized zebrafish eggs (0 days post-fertilization (dpf)) were exposed for five days to CBE (1  $\mu$ M–100 mM) or CP (0.001–100  $\mu$ M) supplemented to the egg water. The larvae were collected, lysed, and analysed by the competitive ABPP method. Exposure to 100 mM CBE was found to reduce ABP labelling of all five glycosidases (**Figure 4A** and **Supplementary Figure 2A**). The  $IC_{50}$  values determined by the competitive ABPP method were: GBA ( $IC_{50}$  = 44.1  $\mu$ M), GBA2 ( $IC_{50}$  = 890  $\mu$ M), GAA ( $IC_{50}$  = 9550  $\mu$ M), GANAB ( $IC_{50}$  = 4700  $\mu$ M) and GUSB ( $IC_{50}$  = 6470  $\mu$ M) (**Supplementary Figure 2A** and **Supplementary Table 1**). Thus, inactivation of GBA in zebrafish larvae takes place 20-fold more avidly than that of GBA2 and 100- to 200-fold more potently than that of GAA, GANAB and GUSB. Analysis of residual enzymatic activity of the various enzymes gave similar results (**Supplementary Figure 2B**). Analysis by enzymatic assay revealed that exposure of the animals to 10 mM CBE did not lead to significant inactivation of other glycosidases ( $\alpha$ - and  $\beta$ -mannosidase, *N*-acetyl  $\alpha$ -galactosidase,  $\beta$ -hexosaminidase,  $\alpha$ -fucosidase and  $\alpha$ -iduronidase) except for  $\beta$ -galactosidase ( $IC_{50}$  = 11.2 mM) and  $\alpha$ -galactosidase ( $IC_{50}$  = 22.5 mM) (**Supplementary Figure 2B**). Exposure of zebrafish to CP (5 days at 1–100  $\mu$ M) also comparably competed GBA and GBA2 labelling, but not that of GUSB, GAA and GANAB (**Figure 4B**). This finding was again supported by results obtained from measurement of residual enzymatic activities (**Supplementary Figure 2B**).

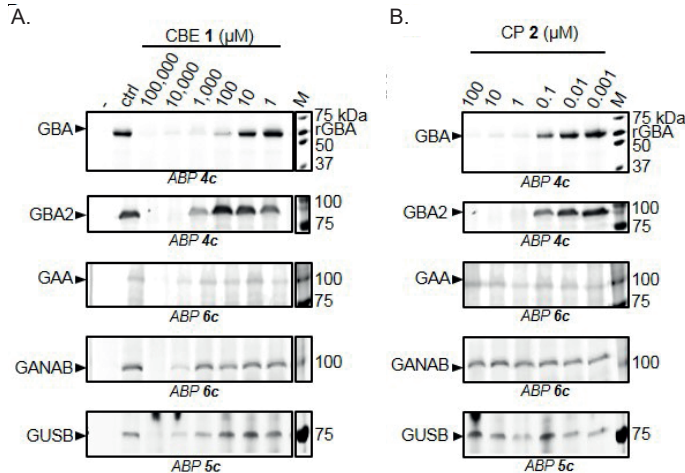


**Figure 4 | *In vivo* glycosidase targets of CBE and CP in developing zebrafish larvae**

Zebrafish embryos were incubated with (A) CBE 0.001–10 mM or (B) CP (0.001–100  $\mu$ M) from 8–120 hours before lysis and subjection to ABP labelling with appropriate ABPs.

### Potency and selectivity of functionalized cyclophellitol inhibitors

From the noted lack of selectivity of CP with respect to inactivation of GBA and GBA2, it is obvious that CP does not allow generation of specific GBA-deficiency in cell and animal models. Functionalized cyclophellitol compounds bearing a fluorescent moiety at C8 have been described as highly potent and selective inhibitors for GBA<sup>28</sup>. Cyclophellitols bearing a simple but bulky hydrophobic moiety at C8, either a biphenyl (compound **3d**) or adamantyl moiety (compound **3e**) were synthesized to generate superior potent and selective GBA inhibitors, with the potential ability to penetrate the brain.

First, the *in vitro* activity and selectivity of these two functionalized cyclophellitol compounds were evaluated towards GBA and the two major off-target glycosidases of CBE and CP: GBA2 and GAA. The inhibitors were preincubated with recombinant human GBA (rGBA, Cerezyme), human GBA2 (from lysates of GBA2 overexpressed cells) and recombinant human GAA (rGAA, Myozyme) for 3 h, followed by enzymatic measurements. Both compound **3d** and **3e** were nanomolar inhibitors of rGBA ( $IC_{50} = 1.0$  nM), which were 4000-fold more potent than CBE **1** (Table 1). In contrast to CBE and CP, both compound **3d** and **3e** were rather inactive toward GBA2 and GAA ( $IC_{50} > 100$   $\mu$ M), thus making them 4000 times and 200 times more selective than for example CBE **1** ( $IC_{50}$  ratio = 23.6 for GBA2/GBA and 444 for GAA/GBA, Table 1).

**Table 1** | Apparent  $IC_{50}$  values for *in vitro* inhibition of GBA, GBA2 and GAA in recombinant enzymes (rGBA and rGAA) or overexpressed cell lysates (GBA2) by compounds CBE 1, CP 2, ABP 3a, ABP 3c, 3d and 3e measured as residual glycosidase activity. Error ranges depict standard deviations from biological triplicates.

<i>In vitro</i>	CBE 1 (nM)	CP 2 (nM)	ABP 3a (nM)	ABP 3c (nM)	3d (nM)	3e (nM)
<b>rGBA</b>	4,280 ± 500	29.6 ± 2.40	1.20 ± 0.30	3.20 ± 0.17	1.06 ± 0.19	0.96 ± 0.17
<b>GBA2</b> (HEK293T lysates)	101,000 ± 20,100	29.7 ± 3.13	> 10 <sup>5</sup>	412,000 ± 10,100	> 10 <sup>5</sup>	> 10 <sup>5</sup>
<b>rGAA</b>	1,900,000 ± 192,000	> 10 <sup>5</sup>	> 10 <sup>5</sup>	> 10 <sup>5</sup>	> 10 <sup>5</sup>	> 10 <sup>5</sup>
<b>Ratio (<i>in vitro</i>)</b>						
GBA2/ GBA	24	1	> 10 <sup>5</sup>	> 10 <sup>4</sup>	> 10 <sup>5</sup>	> 10 <sup>5</sup>
GAA/ GBA	444	> 10 <sup>3</sup>	> 10 <sup>6</sup>	> 10 <sup>6</sup>	> 10 <sup>6</sup>	> 10 <sup>6</sup>

As for CBE **1** and CP **2**, the *in vivo* activity of compounds **3d** and **3e** was evaluated by addition of the compounds to the swimming water of developing zebrafish embryos. After 5 days of incubation at 28 °C, larvae were homogenized and enzyme selectivity was analysed by appropriate competitive ABP labelling. Quantification of ABP-labelled bands revealed that compounds **3d** and **3e** had *in vivo* apparent  $IC_{50}$  values towards GBA of 4-6 nM and that they were 5-70-fold more potent than ABP **3a** or **3c** and 7500-fold more potent than CBE **1** (Table 2). Potential off-target glycosidases such as GBA2, LPH, GAA, GANAB and GUSB were not identified with compounds **3d** and **3e**<sup>36</sup>.

**Table 2 |** Apparent  $IC_{50}$  values for *in vivo* inhibition in 5-day treated zebrafish embryos with compounds 1, 2, 3a, 3c, 3d and 3e as evaluated by quantification of residual labelling using appropriate ABPs. Error ranges depict standard deviations from n = 12-24 individuals.

<i>In vivo</i> <i>Danio rerio</i> larvae	CBE 1 (nM)	CP 2 (nM)	ABP 3a (nM)	ABP 3c (nM)	3d (nM)	3e (nM)
<b>GBA</b>	$4.41 \times 10^4$	83	$31.6 \pm 8.88$	$284 \pm 31.5$	$5.85 \pm 2.44$	$3.94 \pm 0.21$
<b>GBA2</b>	$8.90 \times 10^5$	59	$> 10^4$	$> 10^4$	$> 10^4$	$> 10^4$
<b>GAA</b>	$9.55 \times 10^6$	$> 10^5$	$> 10^4$	$> 10^4$	$> 10^4$	$> 10^4$
<b>Ratio (<i>in vivo</i>)</b>						
GBA2/ GBA	22	0.714	$> 316$	$> 35$	$> 1710$	$> 2540$
GAA/ GBA	233	$> 120$	$> 316$	$> 35$	$> 1710$	$> 2540$

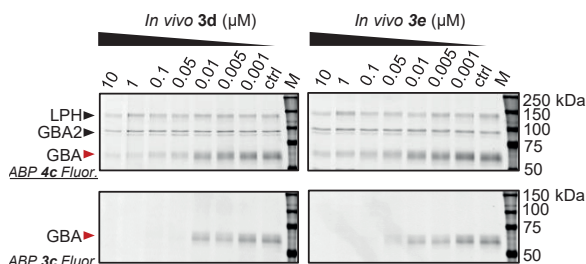


**Figure 5 |** *In vivo* glycosidase targets of compounds 3d and 3e in developing zebrafish larvae.

Zebrafish embryos were incubated with compound 3d and 3e (0.001-10  $\mu$ M) from 8-120 hours before lysis and subjection to ABP labelling with broad-spectrum retaining  $\beta$ -glucosidase ABP 4c, targeting GBA, GBA2 and LPH, and selective GBA ABP 3c as readout.

### Impact of inhibitors on glycosphingolipids accumulation in treated zebrafish larvae

Next the functional impact of the GBA inhibitors was evaluated by exposing embryos for 5 days to CBE, CP or the functionalized CP compounds. *In vivo* inactivation of GBA leads to compensatory formation of glucosylsphingosine (GlcSph) by acid ceramidase-mediated conversion of accumulating GlcCer in lysosomes and such accumulation of GlcSph is a biomarker of the inactivation of GBA<sup>33,37</sup>. The exposure of zebrafish larvae to CBE 1, CP 2 and functionalized cyclophellitol ABP 3a and compounds 3d and 3e led to pronounced accumulation of GlcSph. A 4-fold increase in the case of 1000  $\mu$ M CBE 1 and 6-fold increase at 10  $\mu$ M CP 2 was observed while ABP 3a and inhibitors 3d and 3e reached a 10-30-fold elevation in the level of GlcSph using only 0.1-10  $\mu$ M of inhibitor (Figure 6). Thus, the observed *in vivo* target engagement of GBA according to ABP detection was confirmed by the accumulation of GlcSph at comparable inhibitor concentrations. However, reaching similar GlcSph levels in the zebrafish with CBE 1 required 100-10000-fold higher concentration in contrast to compounds 3d and 3e, concentrations at which GBA2 and GAA may also be targeted (Figure 4 and Table 2).

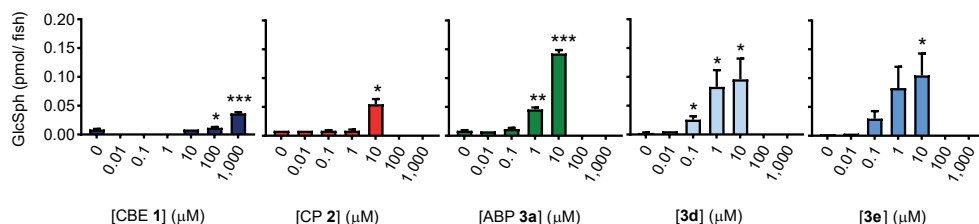


**Figure 6 |** Glucosylsphingosine levels in zebrafish embryos treated for 5 days with inhibitors CBE **1**, CP **2**, ABP **3a**, compounds **3d** or **3e**. Error ranges depict standard deviations from  $n = 3$  individuals. \*  $P < 0.5$ , \*\*\*  $P < 0.001$ .

### Brain permeability of functionalized cyclophellitol inhibitors

Finally, brain penetration of the new cyclophellitol inhibitors was evaluated, a crucial feature for their future application in the study of neuropathic Gaucher disease and Parkinson's disease. Adult zebrafish of 3 months' age were treated with DMSO, ABP **3a** or compound **3e** (1.6 nmol/fish, approximately 4 μmol/kg) administered via food intake, and after 16 h brains and other organs were isolated, homogenized, and analysed by ABP labelling using appropriate ABPs for GBA, GBA2, GAA, GANAB and GUSB. Labelling of brain homogenate of adult zebrafish with ABP **3c** resulted in considerable GBA labelling in control and ABP **3a** treated fish, but no labelling in brain homogenates from fish treated with compound **3e** (Figure 7A).

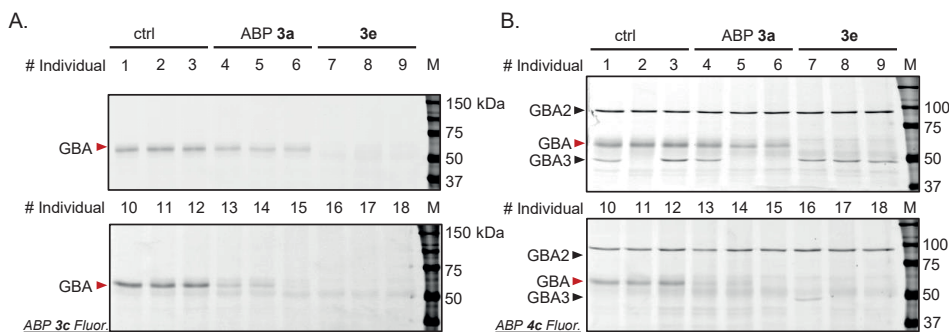


**Figure 7 |** In vivo targets of functionalized cyclophellitols in zebrafish adult brain

Adult zebrafish were treated with DMSO, ABP **3a** or compound **3e** and *in vivo* target engagement was visualized by labelling with (A) selective GBA ABP **3c** or (B) broad-spectrum retaining β-glucosidase ABP **4c** labelling GBA, GBA2 and GBA3.

Labelling by the broad-spectrum β-glucosidase ABP **4c** showed that GBA2 was not a target of compound **3e** (Figure 7B), nor was the lower running band (48 kDa), which we hypothesize to be the cytosolic β-glucosidase, GBA3. We noted that the expression level of this protein is likely variable among individual fish, as 4 out of 6 fishes in the control group lacked this band. ABP labelling of other glycosidase targets, such as GAA, GANAB and GUSB, were not affected either<sup>36</sup>. In the visceral organs (both liver and spleen), both ABP **3a** and compound **3e** selectively abrogated GBA while not affecting the labelling of other tested glycosidases (Supplementary Figure 3 and ref. 36).

## Discussion

Zebrafish offer attractive features for pharmacological screenings. Hundreds of fertilized eggs can be easily obtained and their ex-vivo, rapid embryogenesis and organ development as well as small size have enabled researchers to study the effects of various small molecules in a whole organism in a relatively high throughput manner<sup>38,39</sup>. Off-target effects can have detrimental consequences, not only in the process of drug discovery and development but also in fundamental research when pharmacological modulation is used to study the molecular basis of a human disorder in a model organism. On-demand GBA deficiency has been used to study GD in mouse models, however concerns about potential off-target effects have been raised when using high concentrations of the established GBA selective inhibitors CBE and CP. In the present study, developing zebrafish larvae were used to determine the *in vivo* potency of CBE and CP as well as in-house synthesized CP derivatives and to evaluate their dose-dependent target engagement.

First of all, it is noteworthy to mention that the same tools can be used for the study of glycosidases in zebrafish as for cellular and mouse samples. In chapter 2 it was shown that the catalytic features of zebrafish GBA could be studied using the artificial 4MU- $\beta$ -Glc substrate and this chapter revealed that it was possible to evaluate enzymatic activity of other glycosidases by use of their corresponding fluorogenic substrates. In addition, the library of fluorescent ABPs provide a complementary method for activity assessment and visualization of active retaining glycosidases. The ABPs bind in a mechanism-based manner and the required nucleophilic and acid base residues are generally conserved across species. Therefore ABPs have not only been found to react with retaining glycosidases of mammals, but also with those from zebrafish, plants, bacteria and fungi<sup>30,40-42</sup>. In contrast, none of the in-house available commercial glycosidase antibodies were found to react with the respective enzyme from zebrafish materials, including tested antibodies for GBA, GBA2,  $\alpha$ -galactosidase A and galactocerebrosidase (data not shown). Modification of the reporter tag of the ABP enables researchers to visualize active enzyme by means of a fluorescent tag in combination with in-gel fluorescence scanning or fluorescence microscopy<sup>28,29</sup>, while affinity tags allows the enrichment and identification of target enzymes by chemical proteomics approaches<sup>43</sup>. Zebrafish research could profit extensively from the use of ABPs. Mechanism-based ABPs, as well as affinity-based ones, have been developed for other enzyme classes including serine hydrolases<sup>44,45</sup>, kinases<sup>46</sup>, proteases<sup>47</sup> and subunits of the proteasome<sup>48</sup>.

Another advantage is that the ABP only reacts with an active enzyme, thereby enabling evaluation of selectivity and potency of small molecules by an approach called competitive activity-based protein profiling (cABPP). This approach was adopted in this study to verify the use of zebrafish larvae as whole organismal model to study target engagement of GBA inhibitors. The apparent  $IC_{50}$  values of zebrafish larvae were compared to those obtained in cultured cells, using both activity measurements with fluorogenic substrates as well as cABPP in parallel.

In general, inhibitors were approximately 5-fold more potent in cultured cells compared to developing zebrafish larvae (CBE: 0.6  $\mu\text{M}$  vs 44  $\mu\text{M}$  and CP: 15 nM vs 83 nM for cultured cells and zebrafish larvae respectively). The observed selectivity of CBE and CP was similar in cultured cells and developing zebrafish larvae. Non-lysosomal  $\beta$ -glucosidase GBA2 and the lysosomal  $\alpha$ -glucosidase GAA were determined as off-targets of CBE both in cultured cells overexpressing GBA2 and in developing zebrafish larvae upon incubation with high concentrations of CBE. A selective window for *in vivo* GBA inactivation was apparent of 0.6-315  $\mu\text{M}$  for cultured cells and 44-890  $\mu\text{M}$  for zebrafish larvae (**Figure 8**). Such selectivity has also been observed in brain of mice treated with a low and high concentrations of CBE<sup>35</sup>. CP showed potent GBA inactivation both in cultured cells and zebrafish larvae, however this compound also inactivated GBA2 with comparable potency. Therefore this inhibitor presents a small GBA selective window for cultured cells and none for zebrafish larvae (**Figure 8**).

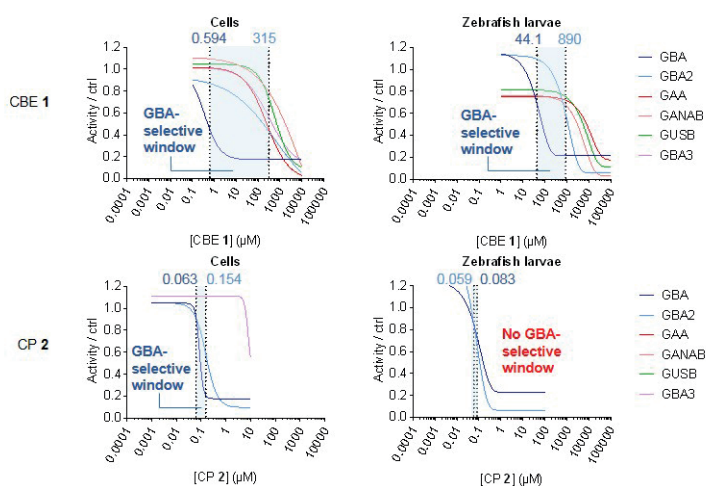


**Figure 8 | Window for selective GBA inhibition by CBE and CP in cultured cells and zebrafish larvae.**

Inhibition curves for CBE or CP towards GBA and other glycosidases were derived from the results of ABP detection (average of  $n = 3$  biological replicates). The GBA selective window is depicted as the blue area between the two dotted lines and defined as the concentration range for CBE or CP between its  $\text{IC}_{50}$  values towards GBA and the next major glycosidase target (in all cases, GBA2).

The CP derivatives, functionalized at C8 with a BODIPY (**3a**), biphenyl (**3d**) or adamantyl (**3e**), displayed both a very high potency and selectivity for GBA inactivation in developing zebrafish larvae. Apparent  $\text{IC}_{50}$  values of 4-31 nM were determined and no subsequent effect on *in vitro* ABP labelling of GBA2, LPH, GAA, ER  $\alpha$ -glucosidase GANAB or lysosomal  $\beta$ -glucuronidase (GUSB) even at high concentrations of inhibitor ( $>10 \mu\text{M}$ ). Overall, these results show comparable *in vivo* potency and selectivity in cultured cells and developing zebrafish larvae. A slightly higher potency was again observed using cultured cells, however this could be explained by the route of administration, possible storage of the small molecule in the lipid- and protein rich environment of the yolk (unpublished observations of Wouter Kallemeijn) as well as the complexity of the zebrafish embryo which includes different cell types.

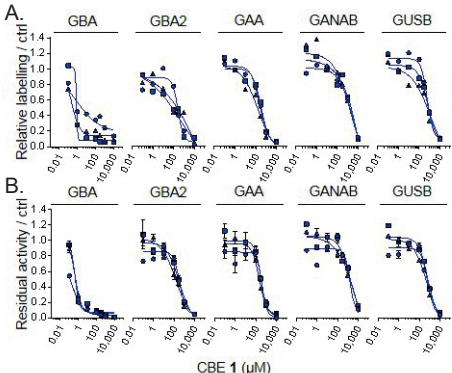


Next, the physiological impact of GBA inactivation was studied by glycosphingolipid analysis. Inhibitor treated zebrafish revealed accumulation of GlcSph, a biochemical biomarker of *in vivo* inactivation of lysosomal GBA. Only a minor significant increase in GlcSph was observed when high concentrations of CBE (1000  $\mu$ M) and CP (10  $\mu$ M) were used, while the CP derivatives significantly increased GlcSph levels already at low concentrations (0.1-1  $\mu$ M). GlcSph levels are also highly elevated in human GD patients<sup>49</sup>, mouse GD models<sup>50</sup> and zebrafish genetic *gba* knockouts (Chapter 5<sup>51</sup>). In the latter study it became obvious that incubation with a relatively high concentration (10  $\mu$ M) of the CP derivative **3e** showed higher GlcSph levels as compared to the genetic *gba*<sup>-/-</sup> larvae. It became apparent that genetic *gba* KO larvae have maternally derived GBA enzyme in their early life, which was also inactivated by treatment with compound **3e**<sup>51</sup>. Due to the easy and throughput administration, compound **3e** is used extensively throughout this thesis to study GBA deficiency in a variety of genetic backgrounds. In addition, no genotyping of the off-spring is necessary, as for the genetic *gba* zebrafish in chapter 5, and all treated off-spring have a GBA deficiency. This could accelerate and simplify the process of sample preparation at 5 dpf.

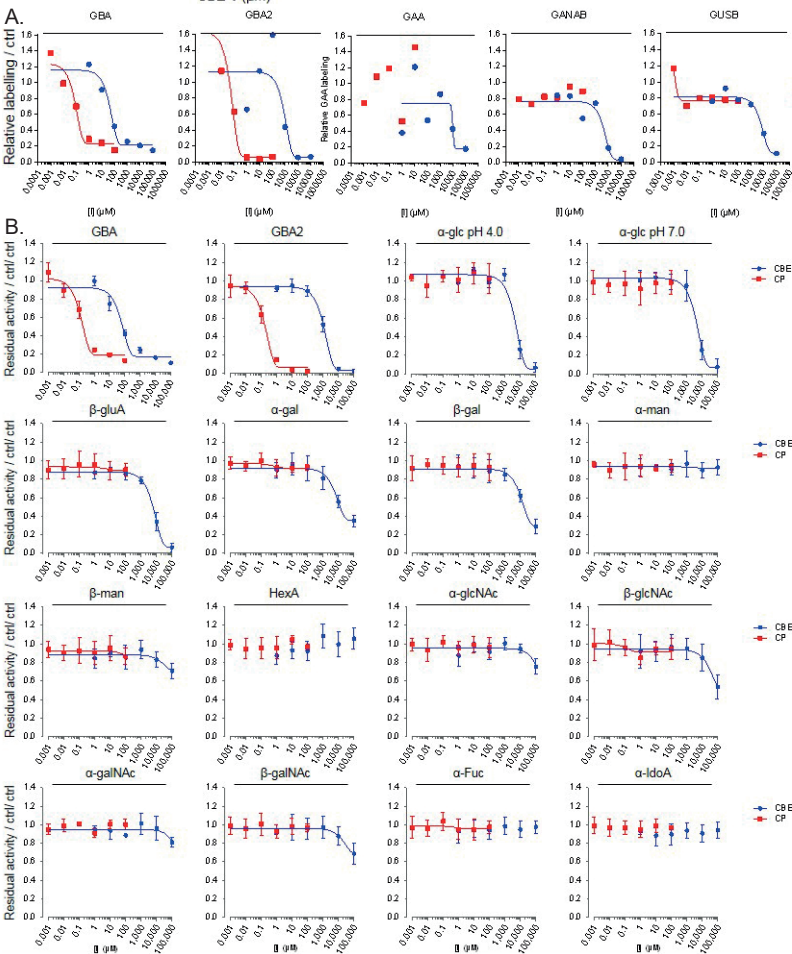
The use of the selective and potent BODIPY functionalized ABP **3a** has been hampered by its inability to inactivate GBA in the brain<sup>29</sup>. As final part of the present study, the newly synthesized CP derivatives were administered to adult zebrafish to evaluate their brain penetration. As expected, ABP **3a** showed inactivation of GBA activity in the spleen and liver but limited inactivation of GBA in the brain, as has already been observed in mice<sup>29,36</sup>. The limited penetration into the brain of the BODIPY ABP can be likely attributed to active removal via Pgp proteins<sup>52</sup>. Compound **3e**, on the other hand, showed complete inactivation of GBA in the liver, spleen and brain without inhibition of off-target proteins. Of note, the CP derivative modified with a Cy5 molecule at C8 (**3c**) was a very potent inhibitor of GBA *in vitro* and in developing zebrafish larvae, however no inactivation of GBA was neither found in brain, liver or spleen and accumulation in the gut was observed (unpublished data).

In conclusion, this study has shown that both zebrafish larvae and adult zebrafish are helpful models to evaluate the potency and target engagement of small molecule inhibitors of GBA. In addition, it has determined that compound **3e** is a superior GBA inhibitor enabling generation of a GBA deficiency, both on-demand in the brain and without any off-target effects, to assist research in the context of neuropathic GD and PD.

Supplementary information



**Supplementary Figure 1 |**  
(A) Quantification of relative ABP labelling of GBA, GBA2, GAA, GANAB and GUSB in lysates of cells treated *in vivo* for 24 h with CBE. (B) Residual activity of glycosidases in cell lysates treated *in vivo* with CBE. Error ranges =  $\pm$  SD, n = 3 (technical replicates).

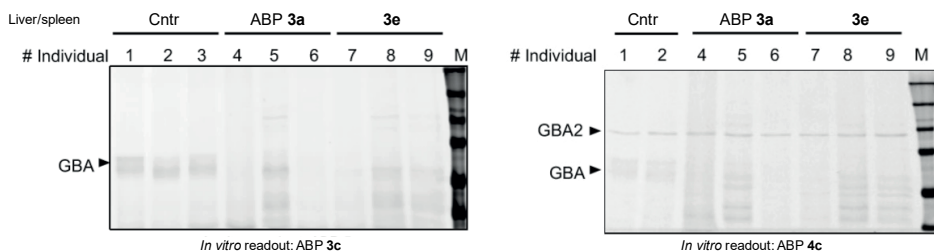


**Supplementary Figure 2 | In vivo incubation with CBE and CP in zebrafish larvae**  
(A) Quantification of gels from Figure 4. (B) Residual activity of glycosidases by enzymatic assay. Error range =  $\pm$  SD, n = 2 technical replicates

**Supplementary Table 1 | *In vivo* target engagement of CBE and CP in cultured cells and zebrafish larvae.**

Cultured cells were incubated for 24 hours and developing zebrafish for 5 days. Apparent  $IC_{50}$  values ( $\mu M$ ) were derived biological triplicate incubations as measured by quantification of *in vitro* ABP labelling on residual active enzymes. – indicates no inhibition at the tested concentrations. Error ranges =  $\pm$  SD, n = 3 biological replicates.

Enzyme	CBE 1 ( $\mu M$ )		CP 2 ( $\mu M$ )	
	Cultured cells	ZF larvae	Cultured cells	ZF larvae
GBA	$0.59 \pm 0.3$	44.1	$0.063 \pm 0.026$	0.083
GBA2	$315 \pm 63$	890	$0.154 \pm 0.07$	0.059
GAA	$249 \pm 84$	9550	–	–
GANAB	$2900 \pm 1120$	4700	–	–
GUSB	$857 \pm 341$	6470	–	–

**Supplementary Figure 3 | *In vivo* targets of ABP 3a and compound 3e in adult liver/spleen.**

DMSO (cntr) or compound soaked food was administered to adult zebrafish and *in vivo* target engagement was visualized by *in vitro* labelling of liver/spleen homogenates with selective GBA ABP 3c (left) or broad-spectrum retaining  $\beta$ -glucosidase ABP 4c labelling GBA, GBA2 and GBA3 (right).

## Experimental procedures

**General materials and methods** - Cyclophellitol (CP), the CP derivatives **3d** and **3e** and the ABPs **3a-c**, **4**, **5** and **6** were synthesized as described earlier<sup>28,30,32,36,53</sup>. Chemicals were obtained from Sigma-Aldrich (St. Louis, MO, USA) if not otherwise indicated. Conduritol B-epoxide (CBE) was purchased from Enzo Life Sciences (Farmingdale, NY, USA). Recombinant GBA (rGBA, imiglucerase) and recombinant human GAA (rGAA, alglucosidase alfa, Myozyme) were obtained from Sanofi Genzyme (Cambridge, MA, USA). HEK293T cells overexpressing human GBA2 were generated as previously described<sup>54</sup> and cultured in DMEM medium (Sigma-Aldrich) supplied with 10% (v/v) FCS, 0.1% (w/v) penicillin/streptomycin, and 1% (v/v) Glutamax, under 5% CO<sub>2</sub>.

**Zebrafish housing and embryo incubations** – Zebrafish were housed at the University of Leiden, the Netherlands, according to standard protocols (zfin.org). The breeding of fish lines was approved by the local animal welfare committee (Instantie voor dierwelzijn, IvD, Leiden). Adults, embryos and larvae were kept at a constant temperature of 28.5 °C. Embryos and larvae, before the free-feeding stage, not falling under animal experimentation law according to the EU animal protection Directive 2010/63/EU, were raised in egg water (60 µg L<sup>-1</sup> sea salt, Sera marin). Synchronized wild-type ABTL zebrafish embryos were acquired after mating of single male and female couples (both > 3 months old) and incubated with appropriate inhibitors as described below.

**Preparation of homogenates** - Homogenates of cells and zebrafish were prepared by lysis in potassium phosphate lysis buffer (25 mM KH<sub>2</sub>PO<sub>4</sub>-K<sub>2</sub>HPO<sub>4</sub>, pH 6.5, protease inhibitor cocktail (EDTA-free, Roche, Basel, Switzerland) and supplemented with 2.5 U/mL benzonase for HEK293T cell homogenates). Cell pellets from two 15-cm culture dishes were resuspended in 1200 µL lysis buffer, while 4µL lysis buffer was used to homogenize 1 zebrafish larvae. Homogenates were prepared by sonication with a Polytron PT 1300D sonicator (Kinematica, Luzern, Switzerland) on ice at 20% power for 3 times 3 s (zebrafish) or passed through a 30-gauge needle 10 times using a 1 mL syringe (HEK293T cells overexpressing GBA2). Protein concentration was measured using Pierce BCA assay kit (Thermo Fisher Scientific, Waltham, MA, USA).

**Enzymatic assays** - All assays were performed in 96-well plates at 37 °C for human and zebrafish materials. For measurements in rGBA or rGAA, 3.16 ng of rGBA enzyme or 2.1 ng rGAA enzyme, while for *in-vitro* measurements in GBA2-overexpressing cell lysates, 8 volumes of cell lysates (7µg total protein/ µL) was used and firstly pre-incubated with 1 volume of ABP **3a** (100 nM final concentration, 0.5% (v/v) DMSO) for 30 min at 37 °C to selectively inhibit GBA activity.

Samples were incubated with compounds (CBE **1**, CP **2**, ABP **3a**, ABP **3c**, **3d** or **3e**) in a final volume of 25 µL, at pH appropriate for each enzyme, while DMSO concentration was kept at 1% (v/v) in all assays during incubation with compounds. Assays were performed by incubating the samples with 100 µL 4MU- (4-methylumbelliferyl-) substrates diluted in McIlvaine buffer (150 mM citric acid—Na<sub>2</sub>HPO<sub>4</sub>, 0.1% (w/v) bovine serum albumin) for a period of 30 min to 2 h and performed in duplicate sets, with 3 replicates at each inhibitor concentration. After stopping the substrate reaction with 200 µL 1M NaOH-glycine (pH 10.3), 4MU-emitted fluorescence was measured with a fluorimeter LS55 (Perkin Elmer, Waltham, MA, USA) using λ<sub>ex</sub> 366 nm and λ<sub>em</sub> 445 nm<sup>28</sup>. Measured activities were subtracted with background values (from samples without enzyme), normalized with the average values from the control samples (no inhibitor), and curve-fitted to inhibitor concentrations using Prism 7.0 (Graphpad) by the [inhibitor] vs response— various slope (four parameters) method to obtain IC<sub>50</sub> values. The substrate mixtures used for each enzyme are listed as follows: GBA, 3.75 mM 4MU-β-D-glucopyranoside (Glycosynth, Warrington Cheshire, UK) at pH 5.2, supplemented with 0.2% (w/v) sodium taurocholate and 0.1% (v/v) Triton X-100, and 25 nM *N*-(5-adamantane-1-ylmethoxy-pentyl)-deoxynojirimycin (AMP-DNM), a GBA2-specific inhibitor<sup>55</sup>; GBA2, 3.75 mM 4MU-β-Dglucopyranoside at pH 5.8, with pre-incubation with 1 µM ABP **3a** for 30 min to specifically inhibit GBA activity; α-glucosidases, 3 mM 4MU-α-D-glucopyranoside at pH 4.0 (GAA) or at 7.0 (GANAB), GUSB, 2 mM

4MU- $\beta$ -D-glucuronide at pH 5.0;  $\alpha$ -galactosidases, 2 mM 4MU- $\alpha$ -D-galactopyranoside at pH 4.6;  $\beta$ -galactosidases, 1 mM 4MU $\beta$ -D-galactopyranoside at pH 4.3 with 0.2 M NaCl;  $\alpha$ -mannosidases, 10 mM 4MU- $\alpha$ -D-mannopyranoside at pH 4.0;  $\beta$ -mannosidases, 2 mM 4MU- $\beta$ -D-mannopyranoside (Glycosynth) at pH 4.2;  $\beta$ -hexosaminidase HexA, 5 mM 4MU- $\beta$ -D6-sulpho-2-acetamido-2-deoxy-glucopyranoside at pH 4.4;  $\beta$ -hexosaminidases HexA/B, 5 mM 4MU- $\beta$ -N-acetylglucosaminide at pH 4.5;  $\alpha$ -N-acetyl-galactosaminidase, 1 mM 4MU- $\alpha$ -N-acetyl-galactosaminide at pH 4.5;  $\alpha$ -L-fucosidase, 1 mM 4MU- $\alpha$ -L-fucopyranoside at pH 5.0,  $\alpha$ -L-iduronidase, 2 mM 4MU- $\alpha$ -L-iduronide (Glycosynth) at pH 4.0; GBA3, 3.75 mM 4MU- $\beta$ -D-glucopyranoside at pH 6.0.

**Fluorescent ABP labelling and detection** - Residual active, not irreversibly inhibited glycosidases were labelled with excess fluorescent ABPs in the optimum McIlvaine buffer, if not otherwise stated (see above). ABP labelling was performed at 37 °C for 30 min for all materials, in a total sample volume of 20–40  $\mu$ L and 0.5–1% DMSO concentration. GBA was labelled with 200 nM ABP **3b** (pH 5.2, 0.1% (v/v) Triton-100, 0.2% (w/v) sodium taurocholate), or labelled together with GBA2 using 200 nM  $\beta$ -aziridine ABP **4c** at pH 5.5. GBA2 was labelled with 200 nM  $\beta$ -aziridine ABP **4a**, **4b** or **4c**. The  $\alpha$ -glucosidases GAA and GANAB were first pre-incubated with 200 nM ABP **4a** for 30 min (pH 4.0 for GAA and pH 7.0 for GANAB), followed by labelling with 500 nM ABP **6a** or **6c** at pH 4.0 or 7.0. The  $\beta$ -glucuronidase GUSB was preincubated with 200 nM ABP **4a** for 30 min, followed by labelling with 200 nM  $\beta$ -aziridine ABP **5c**. After ABP incubation, proteins were denatured by boiling the samples with 5 $\times$  Laemmli buffer (50% (v/v) 1 M Tris-HCl, pH 6.8, 50% (v/v) 100% glycerol, 10% (w/v) DTT, 10% (w/v) SDS, 0.01% (w/v) bromophenol blue) for 5 min at 98 °C, and separated by electrophoresis on 7.5% or 10% (w/v) SDS-PAGE gels running continuously at 90 V<sup>28,30-32</sup>. Wet slab-gels were scanned on fluorescence using the Typhoon FLA 9500 (GE Healthcare) at  $\lambda_{\text{ex}}$  473 nm and  $\lambda_{\text{em}}$   $\geq$  510 nm for green fluorescent ABP **4a** and **6a**; at  $\lambda_{\text{ex}}$  532 nm and  $\lambda_{\text{em}}$   $\geq$  575 nm for ABP **3b** and **4b**; and at  $\lambda_{\text{ex}}$  635 nm and  $\lambda_{\text{em}}$   $\geq$  665 nm for ABP **4c**, **5c** and **6c**. ABP-emitted fluorescence was quantified using ImageQuant software (GE Healthcare, Chicago, IL, USA) and curve-fitted using Prism 7.0 (Graphpad). After fluorescence scanning, SDS-PAGE gels were stained for total protein with Coomassie G250 and scanned on a ChemiDoc MP imager (Bio-Rad).

***In vivo* effects of CBE and CP in intact cultured cells** - Confluent HEK293T stably expressing human GBA2 were cultured in 12-well plates in triplicates with(out) CBE (0.01–10,000  $\mu$ M) or CP (0.001–10  $\mu$ M) for 24 h at 37 °C. For lysis, cells were washed three times with PBS, subsequently lysed by scraping in potassium phosphate buffer (K<sub>2</sub>HPO<sub>4</sub>–KH<sub>2</sub>PO<sub>4</sub>, 25 mM, pH 6.5, supplemented with 0.1% (v/v) Triton X100 and protease inhibitor cocktail (Roche)), aliquoted, and stored at –80 °C. After determination of the protein concentration, lysates containing equal protein amount (5–20  $\mu$ g total protein per measurement) were adjusted to 12  $\mu$ L with potassium phosphate buffer and subjected to residual activity measurements using enzymatic assay (n = 3 technical replicates for each biological triplicate at each treatment condition) or ABP detection (n = 3 biological replicates) as described above.

***In vivo* effects of inhibitors in living zebrafish larvae** - For in vivo inhibitor treatment, a single fertilized embryo was seeded in each well of a 96-wells plate, and exposed to 200  $\mu$ L egg water supplemented with CBE (1–100,000  $\mu$ M), CP (0.001–100  $\mu$ M), ABP **3a** (0.001–10  $\mu$ M), ABP **5** (0.0001–10  $\mu$ M), inhibitor **3c** (0.001–10  $\mu$ M) or **3e** (0.001–10  $\mu$ M) with a final DMSO concentration of 0.5% (v/v) for 120 hours at 28.5 °C. Per condition, n = 24–48 embryos were used. At 120 hours (5 dpf), larvae were collected, rinsed three times with egg water, fully aspirated, snap-frozen in liquid nitrogen and stored at –80 °C until homogenization in 4  $\mu$ L potassium phosphate buffer per individual zebrafish as described above. Samples containing 20–45  $\mu$ g total protein were subjected to the enzymatic assay described in the previous section or diluted in 14  $\mu$ L lysis buffer, added with McIlvaine buffer at various pHs and subjected to ABP detection at a final volume of 32  $\mu$ L for 30 min at 37 °C using ABP methods described above.

## Chapter 3

*In vivo* activity of inhibitors in adult zebrafish - Surplus wild-type adult zebrafish of 3 months of age were administrated with a single dose of food grain mixed with DMSO, ABP **3a** or inhibitor **3e** (1.6 nmol/fish, approximately 4  $\mu$ mol/kg,  $n = 3$  for each treatment) in  $n = 2$  sets, according to project licence AVD1060020184725,1-04. An initial experiment was performed with 3 adult zebrafish and the effect was confirmed by additional 3 individuals per experimental condition. Zebrafish were sacrificed after 24 h using tricaine methane sulfate (MS222; 250 mg/L), organs were harvested, snap-frozen in liquid nitrogen and stored at  $-80^{\circ}\text{C}$  until use. Food grain consisted of Gemma micro mixed with Gemma diamond (Skretting, Stavanger, Norway). Lysis was performed with 50  $\mu$ L lysis buffer (without benzonase) per sample, and lysates containing 20–60  $\mu$ g total protein were analysed by ABP method for GBA, GBA2, GAA, GANAB, and GUSB.

Sphingolipid extraction and analysis by mass spectrometry in zebrafish larvae - Zebrafish embryos at 8 hpf were seeded in 12-well plates (15 fish/well, 3 mL egg water/well) and treated with CBE **1** (10–1,000  $\mu$ M), CP **2** (0.01–10  $\mu$ M), inhibitor **3d** (0.001–10  $\mu$ M) or **3e** (0.001–10  $\mu$ M) for 120 hours at  $28.5^{\circ}\text{C}$ . Thereafter, zebrafish larvae were washed three times with egg water, and collected in clean screw-cap Eppendorf tubes (three tubes of three larvae per inhibitor concentration). Lipids were extracted and measured according to methods described previously<sup>56</sup>. Briefly, after removing of the egg water, 20  $\mu$ L of 13C-GlcSph<sup>57</sup> from concentration 0.1 pmol/ $\mu$ L in MeOH, 480  $\mu$ L MeOH, and 250  $\mu$ L  $\text{CHCl}_3$  were added to the sample, stirred, incubated for 30 min at RT, sonicated (5 x 1 min in sonication water bath), and centrifuged for 10 min at 15,700 g. Supernatant was collected in a clean tube, 250  $\mu$ L  $\text{CHCl}_3$  and 450  $\mu$ L 100 mM formate buffer (pH 3.2) were added. The sample was stirred and centrifuged, the upper phase was transferred to a clean tube. The lower phase was extracted with 500  $\mu$ L MeOH and 450  $\mu$ L formate buffer. The upper phases were pooled and taken to dryness in a vacuum concentrator at  $45^{\circ}\text{C}$ . The residue was extracted with 700  $\mu$ L butanol and 700  $\mu$ L water, stirred and centrifuged. The upper phase (butanol phase) was dried and the residue was dissolved in 100  $\mu$ L MeOH. 10  $\mu$ L of this sample was injected to the LC-MS for lipid measurement with LC-MS/MS methods described previously<sup>56</sup>. Two-tailed unpaired t-test was performed in Prism 7.0 software (Graphpad) to derive statistical significance, where  $p < 0.05$  was considered significant.



## References

1. Brady R.O., Kanfer J.N., Bradley R.M. and Shapiro D. (1966) Demonstration of a deficiency of glucocerebrosidase-cleaving enzyme in Gaucher's disease. *The Journal of clinical investigation* **45**, 1112-1115.
2. Beutler E. and Grabowski G.A. (2001) Gaucher disease. In *The Metabolic and Molecular Bases of Inherited disease*, Volume III, 8th Edition, C.R. Scriver, A.L. Beaudet, W.S. Sly and D. Valle, eds. (New York: McGraw-Hill), pp. 3635-3668.
3. Legler G. (1966) [Studies on the action mechanism of glycoside splitting enzymes, I. Presentation and properties of specific inhibitors]. *Hoppe Seylers Z Physiol Chem* **345**, 197-214.
4. Vardi A., Zigdon H., Meshcheriakova A., Klein A.D., Yaacobi C., Eilam R.,... and Futerman A.H. (2016) Delineating pathological pathways in a chemically induced mouse model of Gaucher disease. *J Pathol* **239**, 496-509.
5. Legler G. (1990) Glycoside hydrolases: mechanistic information from studies with reversible and irreversible inhibitors. *Adv Carbohydr Chem Biochem* **48**, 319-384.
6. Kacher Y., Brumshtein B., Boldin-Adamsky S., Toker L., Shainskaya A., Silman I.,... and Futerman A.H. (2008) Acid beta-glucosidase: insights from structural analysis and relevance to Gaucher disease therapy. *Biol Chem* **389**, 1361-1369.
7. Premkumar L., Sawkar A.R., Boldin-Adamsky S., Toker L., Silman I., Kelly J.W.,... and Sussman J.L. (2005) X-ray structure of human acid-beta-glucosidase covalently bound to conduritol-B-epoxide. Implications for Gaucher disease. *J Biol Chem* **280**, 23815-23819.
8. Kanfer J.N., Legler G., Sullivan J., Raghavan S.S. and Mumford R.A. (1975) The Gaucher mouse. *Biochem Biophys Res Commun* **67**, 85-90.
9. Manning-Bog A.B., Schule B. and Langston J.W. (2009) Alpha-synuclein-glucocerebrosidase interactions in pharmacological Gaucher models: a biological link between Gaucher disease and parkinsonism. *Neurotoxicology* **30**, 1127-1132.
10. Xu Y.H., Sun Y., Ran H., Quinn B., Witte D. and Grabowski G.A. (2011) Accumulation and distribution of alpha-synuclein and ubiquitin in the CNS of Gaucher disease mouse models. *Mol Genet Metab* **102**, 436-447.
11. Rocha E.M., Smith G.A., Park E., Cao H., Graham A.R., Brown E.,... and Isacson O. (2015) Sustained Systemic Glucocerebrosidase Inhibition Induces Brain alpha-Synuclein Aggregation, Microglia and Complement C1q Activation in Mice. *Antioxid Redox Signal* **23**, 550-564.
12. Newburg D.S., Shea T.B., Yatziv S., Raghavan S.S. and McCluer R.H. (1988) Macrophages exposed in vitro to conduritol B epoxide resemble Gaucher cells. *Exp Mol Pathol* **48**, 317-323.
13. Newburg D.S., Yatziv S., McCluer R.H. and Raghavan S. (1986) beta-Glucosidase inhibition in murine peritoneal macrophages by conduritol-B-epoxide: an in vitro model of the Gaucher cell. *Biochimica et biophysica acta* **877**, 121-126.
14. Prenc E.M., Chaturvedi P. and Newburg D.S. (1996) In vitro accumulation of glucocerebrosidase in neuroblastoma cells: a model for study of Gaucher disease pathobiology. *J Neurosci Res* **43**, 365-371.
15. Bieberich E., Freischutz B., Suzuki M. and Yu R.K. (1999) Differential effects of glycolipid biosynthesis inhibitors on ceramide-induced cell death in neuroblastoma cells. *J Neurochem* **72**, 1040-1049.
16. Berger J., Lecourt S., Vanneaux V., Rapatel C., Boisgard S., Caillaud C.,... and Berger M.G. (2010) Glucocerebrosidase deficiency dramatically impairs human bone marrow haematopoiesis in an in vitro model of Gaucher disease. *Br J Haematol* **150**, 93-101.
17. Schueler U.H., Kolter T., Kaneski C.R., Zirzow G.C., Sandhoff K. and Brady R.O. (2004) Correlation between enzyme activity and substrate storage in a cell culture model system for Gaucher disease. *J Inherit Metab Dis* **27**, 649-658.
18. Lecourt S., Vanneaux V., Cras A., Freida D., Heraoui D., Herbi L.,... and Larghero J. (2012) Bone marrow microenvironment in an in vitro model of Gaucher disease: consequences of glucocerebrosidase deficiency. *Stem Cells Dev* **21**, 239-248.
19. Quaroni A., Gershon E. and Semenza G. (1974) Affinity labeling of the active sites in the sucrase-isomaltase complex from small intestine. *J Biol Chem* **249**, 6424-6433.
20. Yang S.J., Ge S.G., Zeng Y.C. and Zhang S.Z. (1985) Inactivation of alpha-glucosidase by the active-site-directed inhibitor, conduritol B epoxide. *Biochimica et biophysica acta* **828**, 236-240.
21. Hermans M.M., Kroos M.A., van Beeumen J., Oostra B.A. and Reuser A.J. (1991) Human lysosomal alpha-glucosidase. Characterization of the catalytic site. *J Biol Chem* **266**, 13507-13512.
22. van Weely S., Brandsma M., Strijland A., Tager J.M. and Aerts J.M. (1993) Demonstration of the existence of a second, non-lysosomal glucocerebrosidase that is not deficient in Gaucher disease. *Biochimica et biophysica acta* **1181**, 55-62.
23. Ridley C.M., Thur K.E., Shanahan J., Thillaiappan N.B., Shen A., Uhl K.,... and van der Spoel A.C. (2013) beta-Glucosidase 2 (GBA2) activity and imino sugar pharmacology. *J Biol Chem* **288**, 26052-26066.
24. Hara A. and Radin N.S. (1979) Enzymic effects of beta-glucosidase destruction in mice. Changes in

- glucuronidase levels. *Biochimica et biophysica acta* **582**, 423-433.
25. Braun H., Legler G., Deshusses J. and Semenza G. (1977) Stereospecific ring opening of condurititol-B-epoxide by an active site aspartate residue of sucrase-isomaltase. *Biochimica et biophysica acta* **483**, 135-140.
26. Atsumi S., Iinuma H., Nosaka C. and Umezawa K. (1990) Biological activities of cyclophellitol. *J Antibiot (Tokyo)* **43**, 1579-1585.
27. Withers S.G. and Umezawa K. (1991) Cyclophellitol: a naturally occurring mechanism-based inactivator of beta-glucosidases. *Biochem Biophys Res Commun* **177**, 532-537.
28. Witte M.D., Kallemeijn W.W., Aten J., Li K.Y., Strijland A., Donker-Koopman W.E.,... and Aerts J.M. (2010) Ultrasensitive in situ visualization of active glucocerebrosidase molecules. *Nature chemical biology* **6**, 907-913.
29. Herrera Moro Chao D., Kallemeijn W.W., Marques A.R., Orre M., Ottenhoff R., van Roomen C.,... and Aerts J.M. (2015) Visualization of Active Glucocerebrosidase in Rodent Brain with High Spatial Resolution following In Situ Labeling with Fluorescent Activity Based Probes. *PLoS one* **10**, e0138107.
30. Kallemeijn W.W., Li K.Y., Witte M.D., Marques A.R., Aten J., Scheij S.,... and Overkleeft H.S. (2012) Novel activity-based probes for broad-spectrum profiling of retaining beta-exoglucosidases in situ and in vivo. *Angewandte Chemie* **51**, 12529-12533.
31. Wu L., Jiang J., Jin Y., Kallemeijn W.W., Kuo C.L., Artola M.,... and Davies G.J. (2017) Activity-based probes for functional interrogation of retaining beta-glucuronidases. *Nature chemical biology* **13**, 867-873.
32. Jiang J., Kuo C.L., Wu L., Franke C., Kallemeijn W.W., Florea B.I.,... and Aerts J.M. (2016) Detection of Active Mammalian GH31 alpha-Glucosidases in Health and Disease Using In-Class, Broad-Spectrum Activity-Based Probes. *ACS Cent Sci* **2**, 351-358.
33. Dekker N., van Dussen L., Hollak C.E., Overkleeft H., Scheij S., Ghauharali K.,... and Aerts J.M. (2011) Elevated plasma glucosylsphingosine in Gaucher disease: relation to phenotype, storage cell markers, and therapeutic response. *Blood* **118**, e118-127.
34. Aerts J.M., Donker-Koopman W.E., van Laar C., Brul S., Murray G.J., Wenger D.A.,... and Schram A.W. (1987) Relationship between the two immunologically distinguishable forms of glucocerebrosidase in tissue extracts. *Eur J Biochem* **163**, 583-589.
35. Kuo C.L., Kallemeijn W.W., Lelieveld L.T., Mirzaian M., Zoutendijk I., Vardi A.,... and Artola M. (2019) In vivo inactivation of glycosidases by condurititol B epoxide and cyclophellitol as revealed by activity-based protein profiling. *FEBS J* **286**, 584-600.
36. Artola M., Kuo C.L., Lelieveld L.T., Rowland R.J., van der Marel G.A., Codee J.D.C.,... and Overkleeft H.S. (2019) Functionalized Cyclophellitols Are Selective Glucocerebrosidase Inhibitors and Induce a Bona Fide Neuropathic Gaucher Model in Zebrafish. *Journal of the American Chemical Society* **141**, 4214-4218.
37. Ferraz M.J., Marques A.R., Appelman M.D., Verhoek M., Strijland A., Mirzaian M.,... and Aerts J.M. (2016) Lysosomal glycosphingolipid catabolism by acid ceramidase: formation of glycosphingoid bases during deficiency of glycosidases. *FEBS Lett* **590**, 716-725.
38. MacRae C.A. and Peterson R.T. (2015) Zebrafish as tools for drug discovery. *Nature reviews. Drug discovery* **14**, 721-731.
39. Rennekamp A.J. and Peterson R.T. (2015) 15 years of zebrafish chemical screening. *Current opinion in chemical biology* **24**, 58-70.
40. Kytidou K., Beenakker T.J.M., Westerhof L.B., Hokke C.H., Moolenaar G.F., Goosen N.,... and Aerts J. (2017) Human Alpha Galactosidases Transiently Produced in Nicotiana benthamiana Leaves: New Insights in Substrate Specificities with Relevance for Fabry Disease. *Front Plant Sci* **8**, 1026.
41. Kuo C.L., van Meel E., Kytidou K., Kallemeijn W.W., Witte M., Overkleeft H.S.,... and Aerts J.M. (2018) Activity-Based Probes for Glycosidases: Profiling and Other Applications. *Methods Enzymol* **598**, 217-235.
42. Schroder S.P., de Boer C., McGregor N.G.S., Rowland R.J., Moroz O., Blagova E.,... and Overkleeft H.S. (2019) Dynamic and Functional Profiling of Xylan-Degrading Enzymes in Aspergillus Secretomes Using Activity-Based Probes. *ACS Cent Sci* **5**, 1067-1078.
43. van Rooden E.J., Florea B.I., Deng H., Baggelaar M.P., van Esbroeck A.C.M., Zhou J.,... and van der Stelt M. (2018) Mapping in vivo target interaction profiles of covalent inhibitors using chemical proteomics with label-free quantification. *Nat Protoc* **13**, 752-767.
44. Baggelaar M.P., Janssen F.J., van Esbroeck A.C., den Dulk H., Allara M., Hoogendoorn S.,... and van der Stelt M. (2013) Development of an activity-based probe and in silico design reveal highly selective inhibitors for diacylglycerol lipase-alpha in brain. *Angewandte Chemie* **52**, 12081-12085.
45. Liu Y., Patricelli M.P. and Cravatt B.F. (1999) Activity-based protein profiling: the serine hydrolases. *Proc Natl Acad Sci U S A* **96**, 14694-14699.
46. Zhao Q., Ouyang X., Wan X., Gajiwala K.S., Kath J.C., Jones L.H.,... and Taunton J. (2017) Broad-Spectrum Kinase Profiling in Live Cells with Lysine-Targeted Sulfonyl Fluoride Probes. *Journal of the American Chemical Society* **139**, 680-685.

47. Sanman L.E. and Bogoy M. (2014) Activity-based profiling of proteases. *Annu Rev Biochem* **83**, 249-273.
48. Xin B.T., Espinal C., de Bruin G., Filippov D.V., van der Marel G.A., Florea B.I. and Overkleeft H.S. (2020) Two-Step Bioorthogonal Activity-Based Protein Profiling of Individual Human Proteasome Catalytic Sites. *ChemBiochem* **21**, 248-255.
49. Mirzaian M., Wisse P., Ferraz M.J., Gold H., Donker-Koopman W.E., Verhoek M.,... and Aerts J.M. (2015) Mass spectrometric quantification of glucosylsphingosine in plasma and urine of type 1 Gaucher patients using an isotope standard. *Blood Cells Mol Dis* **54**, 307-314.
50. Ferraz M.J., Marques A.R., Gaspar P., Mirzaian M., van Roomen C., Ottenhoff R.,... and Aerts J.M. (2016) Lyso-glycosphingolipid abnormalities in different murine models of lysosomal storage disorders. *Mol Genet Metab* **117**, 186-193.
51. Lelieveld L.T., Mirzaian M., Kuo C.L., Artola M., Ferraz M.J., Peter R.E.A.,... and Aerts J. (2019) Role of beta-glucosidase 2 in aberrant glycosphingolipid metabolism: model of glucocerebrosidase deficiency in zebrafish. *J Lipid Res* **60**, 1851-1867.
52. Fischer S., Kluver N., Burkhardt-Medicke K., Pietsch M., Schmidt A.M., Wellner P.,... and Luckenbach T. (2013) Abcb4 acts as multixenobiotic transporter and active barrier against chemical uptake in zebrafish (*Danio rerio*) embryos. *BMC Biol* **11**, 69.
53. Schroder S.P., van de Sande J.W., Kallemeijn W.W., Kuo C.L., Artola M., van Rooden E.J.,... and Overkleeft H.S. (2017) Towards broad spectrum activity-based glycosidase probes: synthesis and evaluation of deoxygenated cyclophellitol aziridines. *Chemical communications* **53**, 12528-12531.
54. Lahav D., Liu B., van den Berg R., van den Nieuwendijk A., Wennekes T., Ghisaidoobe A.T.,... and Overkleeft H.S. (2017) A Fluorescence Polarization Activity-Based Protein Profiling Assay in the Discovery of Potent, Selective Inhibitors for Human Nonlysosomal Glucosylceramidase. *Journal of the American Chemical Society* **139**, 14192-14197.
55. Overkleeft H.S., Renkema G.H., Neele J., Vianello P., Hung I.O., Strijland A.,... and Aerts J.M. (1998) Generation of specific deoxynojirimycin-type inhibitors of the non-lysosomal glucosylceramidase. *J Biol Chem* **273**, 26522-26527.
56. Mirzaian M., Wisse P., Ferraz M.J., Marques A.R.A., Gaspar P., Oussoren S.V.,... and Aerts J.M. (2017) Simultaneous quantitation of sphingoid bases by UPLC-ESI-MS/MS with identical (13)C-encoded internal standards. *Clin Chim Acta* **466**, 178-184.
57. Wisse P., Gold H., Mirzaian M., Ferraz M.J., Lutteke G., van den Berg R.J.B.H.N.,... and Overkleeft H.S. (2015) Synthesis of a Panel of Carbon-13-Labelled (Glyco)Sphingolipids. *Eur J Org Chem* **2015**, 2661-2677.